The Effect of mild CO_2 Treatment on Thermal Properties of Poly(L-lactic acid): An Experimental Study

Alessandra Longo[1,2,3], Ernesto Di Maio[2,3], Maria Laura Di Lorenzo[*1]

[1]National Research Council (CNR), Institute of Polymers, Composites and Biomaterials (IPCB), c/o Comprensorio Olivetti, Via Campi Flegrei 34, 80078, Pozzuoli, Italy

[2]Dipartimento di Ingegneria Chimica, dei Materiali e della Produzione Industriale, University of Naples Federico II, Piazzale Vincenzo Tecchio, 80, 80125, Naples (NA), Italy

[3]foamlab, University of Naples Federico II, Piazzale Vincenzo Tecchio, 80, 80125, Naples (NA), Italy

Abstract

The influence of mild CO_2 treatment on thermal properties of poly (L-lactic) acid (PLLA) is discussed in this article. A slowly crystallizing PLLA with 4% D-isomer was treated with CO_2 at room temperature and moderate pressures (up to 6.0 MPa) for short times, not longer than 20 minutes. These mild treatments are sufficient to develop ε-form (PLLA/CO_2 complex), which evolves to α"-mesophase after desorption of CO_2. The amount of mesophase depends on the pressure of CO_2 and the sorption times, and significantly affects the thermal properties of PLLA. Although the mesophase melts immediately above the glass transition, it affects subsequent cold crystallization. The influence of CO_2 sorption time and pressure on the cold crystallization kinetics of PLLA is quantified here, and it is found that only a few minutes of treatment with low-pressure CO_2 is sufficient to enhance the crystallization rate. After longer exposure to CO_2, α-crystals also develop, especially under high CO_2 pressure, hence proper adjustment of these parameters can allow tuning the structure and thermal properties of PLLA. The results demonstrate the possibility of producing CO_2-induced mesophase at room temperature using very short sorption times, thus introducing a fast, green and cost-effective way to tailor the crystallization kinetics of PLLA.

Introduction

Poly(L-lactic) acid (PLLA) is a biodegradable polyester of huge industrial interest, with applications ranging from disposable plastics for packaging to foaming for medical engineering [1–6]. Its biocompatibility, biodegradability, and appreciable physical and mechanical properties are governed by crystalline structure and morphology [6–9], including crystallinity [10,11] and polymorphism [12–14]. Crystal modifications of PLLA

* Corresponding author. Email: dilorenzo@ipcb.cnr.it

have been reported to influence mechanical and barrier properties [12–14], and an increase in crystallinity improves thermal stability [15,16], but worsens biodegradation [7,10,17].

The crystallization kinetics of PLLA has been widely studied [18–20]. As it is typical for semicrystalline polymers, crystal morphology and crystallization rate of PLLA are affected by the crystallization path, with huge differences between cold crystallization (i.e., when heated from below the glass transition temperature, T_g), and melt crystallization (i.e., upon cooling from the melt) that have been quantified in dependence on molecular parameters of the polymer [18,21]. The latter mainly include stereoregularity of the chain (ratio of L- and D-isomer, since commercial PLLA grades usually contain 1-4% D-isomer), molar mass [18,22,23], or chain branching [20,24], with data from the literature available for both melt and cold crystallization.

PLLA crystallization is rather slow, compared to most commodity plastics, the slow kinetics of crystallization being probably the main weakness of this polymer: it complicates industrial processing to achieve in due time products with the performance needed in terms of mechanical, thermal and transport properties, attainable only with a sufficiently high degree of crystallinity [16,25]. Large research efforts have been carried out to establish an easy way to adjust the crystalline structure/morphology of PLLA, and different methodologies have been reported, the most common ones being the addition of plasticizers [26–28] or the compounding of the polymer with nucleating additives [26,29,30]. However, the presence of additives in the formulation often negatively impacts biodegradation and biocompatibility of PLLA [31].

Ways to improve the crystallization capacity of PLLA without compounding with external additives include the use of transient plasticizers, such as CO_2 [32–34], structure modification by chain extenders [24,35], blending with oligomeric PLLA [36,37], or proper thermal history tailoring, for example, by annealing at temperatures close to T_g to promote homogeneous crystal nucleation [21,38–40].

Although improving the kinetics of crystallization of PLLA by modification of the chain structure has been shown to be effective in tailoring the properties of the material [20,41,42], this process has the disadvantage of being not easy to adjust quickly. Each chemical modification produces a material with different thermal properties, which means that, when a different crystallization rate is required, a new reaction with different chemicals and parameters needs to be designed and tailored. The ideal situation would be a process that helps tune the crystalline structure/morphology of PLLA in a fast and economical way, such as sample pretreatment or modification of the process parameters.

One of the main features of PLLA crystallization is complex polymorphism [43,44]. Depending on thermal, chemical, and mechanical treatments, PLLA can crystallize into various crystal forms. The most stable crystal structure is named α-form, and develops upon melt or cold crystallization at temperatures above 120 °C, or after solvent evaporation. Stretching PLLA at large strain and high temperatures leads to β-crystals, and epitaxial crystallization upon specific substrate results in formation of γ-crystals [45–47]. PLLA can also develop mesophases, i.e. intermediate structures between amorphous and crystalline phases. Melt or cold crystallization at temperatures below 120 °C results in conformationally disordered (condis) crystals, named α'-, which have chain packing similar to α-form, but slightly larger lattice dimensions, caused by weak specific

carbonyl and methyl interactions, and conformational disorder of the C_α–C dihedral angle [14,48]. Furthermore, PLLA can co-crystallize with CO_2 [49,50] and some organic solvents [17,26,27] to form complex crystals or clathrate structures, often reported as ε-form [47]. When PLLA is exposed to high CO_2 pressures at temperatures below 50 °C, a PLLA/CO_2 complex develops [51], where CO_2 molecules are surrounded by four PLLA chains in the crystal unit cell [49]. Complete removal of CO_2, for example, by desorption at room temperature, leads to the empty form of PLLA/CO_2 complex, known as α"-form [49]. Both PLLA/CO_2 complex and the emptied α"-form are mesophases, with a much looser chain packing compared to the thermally stable α-crystals [47,49].

A PLLA mesophase has also been reported to develop upon tensile drawing at temperatures around 65-90 °C [52–54]. PLLA mesophases, produced by CO_2 or strain, are metastable and transform to the ordered α-phase upon heating above the T_g [55]. Strain-induced and solvent-induced mesophases have been shown to accelerate PLLA crystallization [56,57] after subsequent heating, also affecting crystal morphology [57,58]. In fact, crystallization obtained via CO_2-induced mesophase generally leads to microspherulites or nanorods, depending on temperature and CO_2 pressure, with a transition from microspherulites to rod-like nanostructures occurring around 15 °C under 7-15 MPa of CO_2, and around 30 °C under 3 MPa of CO_2 [59].

Data from the literature on the effect of CO_2-induced mesophase on the crystallization behavior of PLLA are limited to the formation of mesophase after exposure to CO_2 for long times (several hours), and most studies refer to CO_2 treatments at 0 °C [57,58,60], a temperature where the solubility of CO_2 is very high [61], but this also implies obvious technological disadvantages.

With the aim of introducing a convenient process to improve the crystallization kinetics of PLLA, in this work, we report the formation of PLLA mesophase at room temperature and after saturation times with CO_2 of only a few minutes. PLLA samples containing mesophase, whose formation is demonstrated by X-ray and infrared spectroscopy, were studied by thermal analysis to investigate the influence of CO_2 pressure and sorption time on the thermal properties of PLLA.

The mild operating conditions (low pressure, room temperature, short times) adopted in the present work open up the possibility of producing CO_2-induced mesophase in an affordable way. This procedure appeals as an economic and fast process for tuning the mesophase fraction, and thus the crystallization kinetics and morphology of PLLA, using a green and clean technology that does not involve external compounds that may alter polymer purity and, in turn, biodegradability, recyclability and biocompatibility.

Experimental part

Materials

A commercial grade of PLLA with L-isomer content of 96 % and melt flow index of 6 g · $(10\ min)^{-1}$ (at 210 °C, 2.16 kg), grade name PLA Lx175 [62] was kindly provided by Total Corbion (The Netherlands). Before processing, PLLA was dried at 60°C under vacuum overnight. To have a uniform sample size, therefore

reproducible CO_2 sorption rates, PLLA pellets were compression molded with a Carver laboratory press at a temperature of 190 °C for 2 min, without applied pressure, to allow complete melting. After this period, a pressure of about 20 bar was applied for 2 min, then the press plates equipped with cooling coils were cooled to room temperature. Slabs with a thickness of 0.5 mm were obtained, which were then cut into disks of a diameter of 5 mm with a hollow punch.

Sample preparation

The amorphous PLLA was prepared with a PerkinElmer Pyris Diamond DSC, equipped with an Intracooler II as a cooling system. Each 0.5 mm disk was melted at 200 °C for 3 minutes, followed by rapid cooling to 0 °C at the pre-set rate of 100 $K \cdot min^{-1}$. For this specific PLLA grade, this thermal history has been shown to lead to amorphous samples [40].

The amorphous PLLA disks were exposed to CO_2 at various pressures using a batch autoclave named 'minibatch', extensively described in [63]. Grade 4 CO_2 was provided by SOL Group, Italy. All sorption/desorption experiments were conducted at 25 ± 0.5 °C. The samples were placed in the autoclave and CO_2 was injected to reach the desired pressure. The CO_2 pressure ranged from 3.0 to 6.0 MPa, and sorption times (t_s) of 1 - 20 min were used.

Samples are labeled by indicating the processing conditions, i.e., pressure and t_s as *PLLA_pressure_t_s*. For instance, PLLA maintained for 5 min at 3.0 MPa of CO_2 is named *PLLA_3MPa_5min*. After t_s had elapsed, the CO_2 pressure was slowly released (highest rate below 0.1 MPa/s), and the samples were collected from the autoclave and stored at room temperature for 1 -5 months to allow CO_2 desorption [64].

Measurements

CO_2 desorption was evaluated by monitoring the mass evolution of the samples with a Sartorius CP225D-0CE analytical balance (Sartorius, Germany). In some cases (e.g., samples treated with 3.0 MPa or 4.0 and 5.0 MPa for t_s < 20 minutes), 1 month is sufficient for complete desorption of CO_2 (< 0.1 mg, corresponding to a weight fraction < 0.007). Selected samples were subjected to a five-month desorption, as detailed below.

Mesophase formation was monitored by infrared spectroscopy analysis, using a PerkinElmer FTIR Spectrum 100 equipped with a PerkinElmer ATR accessory with a diamond crystal. Each spectrum is an average of 16 individual scans and has been recorded with a resolution of 4 cm^{-1}.

Additional structural information was obtained by X-ray diffraction analysis (WAXD), using a PANalytical X'PertPro diffractometer equipped with a PIXCel 1D detector, under CuKα radiation. Sample spectra were collected in the range 5–40° 2θ, with a step size of 0.013° 2θ and counting time of 20 s per step.

To evaluate the influence of CO_2 induced mesophase on PLLA crystallization, the power compensated DSC described above was also used for thermal analysis of the samples. The thermal properties were analyzed upon heating from 0 to 200 °C at 20 $K \cdot min^{-1}$. The instrument was calibrated in temperature and energy with

high purity indium [65]. To obtain precise heat capacity data from the heat flow rate measurements, each scan was accompanied by a reference empty pan run, with the mass of the aluminum sample pan and the empty reference pan corresponding within 0.03 mg. Dry nitrogen was used as purge gas at a rate of 30 mL·min^{-1}, and each measurement was repeated three times to ensure reproducibility. The experimental heat capacity data were compared with the thermodynamic specific heat (c_p) values of liquid and solid PLLA, collected in the ATHAS (Advanced Thermal Analysis System) Data Bank established by Prof. Bernhard Wunderlich, to whom this article, and the whole Special Issue, is dedicated.

Results and Discussion

As mentioned in the Introduction section, sorption of CO_2 for a few hours leads to a clathrate structure of PLLA, which spontaneously evolves to α"-mesophase with full desorption of the gas [47,49]. As the amount of CO_2 trapped within the polymer affects its structure and, in turn, its thermal properties, the PLLA samples were desorbed for at least one month to ensure the loss of CO_2 prior to analysis. The kinetics of CO_2 desorption is exampled in Figure 1 for one representative PLLA/CO_2 composition (*PLLA_6 MPa_3 min*) in terms of the weight fraction of CO_2 / PLLA as a function of the desorption time. Most CO_2 is quickly desorbed from the polymer within the first six days. After the initial fast decrease, the decay of CO_2 content becomes much slower, with trace amounts of CO_2 present after three months. Five months are sufficient for this specific sample to recover the initial sample weight.

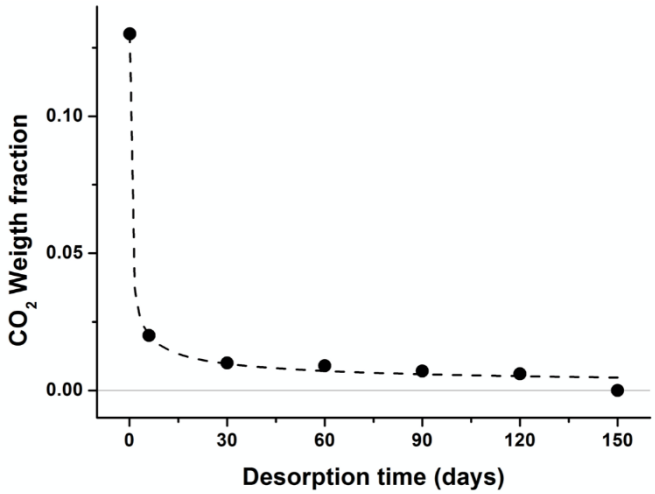

Figure 1. CO_2 desorption curve for the sample *PLLA_6 MPa_3 min* at room temperature and atmospheric ambient pressure (line as a guide for the eye).

The structural analysis of PLLA, after CO_2 treatment and desorption, was carried out by X-ray diffraction and infrared spectroscopy. The WAXD spectra of some selected samples are presented in Figure 2 and compared with literature WAXD spectra of PLLA containing α"-mesophase and ε-clathrate, taken from

Ref. [49]. The α"-mesophase displays a WAXD peak at 2θ = 16.2 °, plus a weaker reflection around 2θ = 22.2 °; in the clathrate ε-structure, the main peak is shifted to 2θ = 14.9 °, with a few weaker reflections that appear at higher 2θ values (18.7 °, 22.3 ° and 24.0 °) [49]. None of these reflections can be disclosed in the WAXD pattern of the *PLLA_3MPa_5min* sample, which only displays a broad halo peaked around 16°, which seems to indicate that the polymer is amorphous. Some degree of order appears in the WAXD spectrum of *PLLA_3 MPa_20 min*, revealed as a weak peak over the amorphous halo at about 15.8 ° (intermediate between emptied α"- and clathrate ε-form), plus a reflection at 2θ = 24 °, typical of the PLLA/CO_2 clathrate [49]. The sorption of CO_2 in *PLLA_4 MPa_5 min* leads to a slightly more ordered structure, with weak reflections that seem to point to the coexistence of both clathrate and α"-mesophase even after prolonged CO_2 desorption at room temperature.

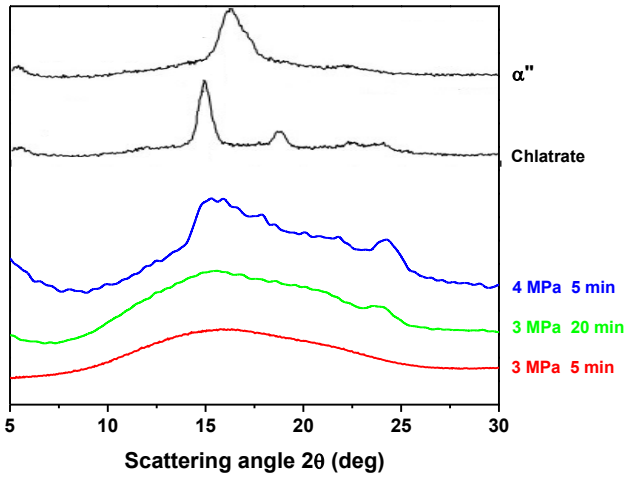

Figure 2. Wide angle X-ray diffraction patterns of PLLA treated with CO_2 at the indicated pressures/times and compared with the WAXD spectra in the literature of PLLA/CO_2 clathrate and α"-mesophase (black plots), adapted from Ref. [49] with permission from Elsevier.

Additional structural characterization of PLLA was conducted after CO_2 sorption and degassing, by infrared spectroscopy. Figure 3 presents the FTIR-ATR spectra of PLLA after CO_2 sorption at various pressures for t_s = 3 min and compared to the fully amorphous polymer (0 MPa). The amorphous PLLA shows no absorption peak in the range of 900 – 930 cm^{-1}, while the FTIR-ATR spectra of PLLA treated with CO_2 show a peak at 918 cm^{-1}, a band typical of PLLA mesophases (including strain-induced mesophase, ε-clathrate and α"-emptied form) [51,56–58], which shifts to slightly higher wavenumber at high CO_2 pressure. The latter indicates presence of also α- or α'-crystals in PLLA treated with high CO_2 pressure: these crystals show an absorbance band at 921-922 cm^{-1}, which is sensitive to the 10_3 helix chain conformation, due to the coupling of the CH_3 rocking mode with the C−C backbone stretching [66]. In other words, Figure 3 reveals that the mesophase is developed in PLLA treated for 3 min with 3.0 – 5.0 MPa of CO_2, with the formation also of ordered crystals with increasing CO_2 pressure, as revealed by the gradual shift to higher wavenumbers of the ATR-FTIR band, whereas 3 min of exposure to 6.0 MPa of CO_2 clearly leads to formation of α'- or α-crystals.

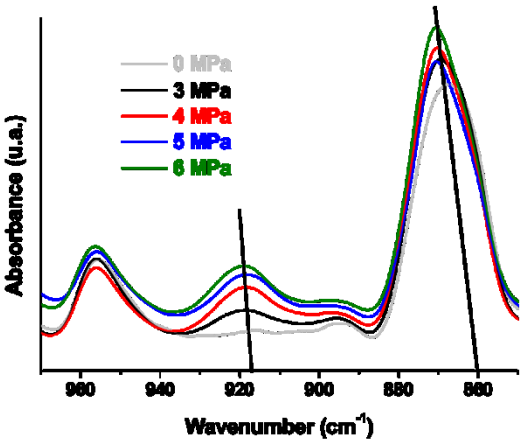

Figure 3. FTIR-ATR spectra of PLLA conditioned with CO_2 at the indicated pressures for 3 min and compared to amorphous PLLA (0.0 MPa).

Treatment with CO_2 for a few minutes induces variations in the FTIR-ATR spectra that are also detectable in the wavelength range between 890 - 850 cm^{-1}, as illustrated in Figure 3. All the analyzed samples showing absorption in the 900 - 930 cm^{-1} range, also present a band around 870 cm^{-1}. The latter is associated with the vibrational mode of C−COO bond [67] and shifts to higher wavenumbers with an increase of CO_2 pressure, similarly to the band at 918 cm^{-1}, further indicating a higher structural order of the polymer with an increase in CO_2 pressure [56,68].

As detailed in Ref. [49], literature WAXD spectra of α"- and ε- mesophases, shown in Figure 2, refer to a PLLA that, after exposure to CO_2 for 2 h at 0 °C, contains 333 mg of CO_2 per g of polymer. Exposure to 3.0 MPa of CO_2 at room temperature for shorter times leads to a much lower fraction of gas within the polymer, which amounts to only 30 mg of CO_2 per g of PLLA, as quantified for the *PLLA_3MPa_5 min* sample immediately after removal from the pressure vessel (1 tenth of the amount reported in Ref. [49]). This explains the limited fraction of mesophase that leads to the absence of clear reflections in the WAXD spectrum compared to the spectra presented in Ref. [49]. Although WAXD analysis of PLLA maintained under CO_2 for a few minutes points to a nearly amorphous polymer, especially at low CO_2 pressures and sorption times, the FTIR-ATR spectra of Fig. 3 clearly prove the formation of a mesophase in PLLA even after exposure to CO_2 at low pressure for a few minutes at room temperature. However, it should be noted that the FTIR-ATR analysis allows the structure of the sample surface to be evaluated at a depth of few μm [69], and does not allow quantitative analysis of the amount of mesophase within the samples.

The thermal properties of PLLA exposed to CO_2 were analyzed by differential scanning calorimetry (DSC). As before, the experimental data refer to samples after CO_2 desorption at room temperature. Figure 4 collects the apparent heat capacity curves of CO_2 treated PLLA for various t_s, grouped by pressure (from 3.0 to 6.0 MPa), together with the apparent c_p plot of quenched PLLA, reported in Figure 4a as "0min" sample.

Further comparison of the heat capacity plots of PLLA samples that are kept at various pressures for the same t_s = 1 min is presented in Figure 5.

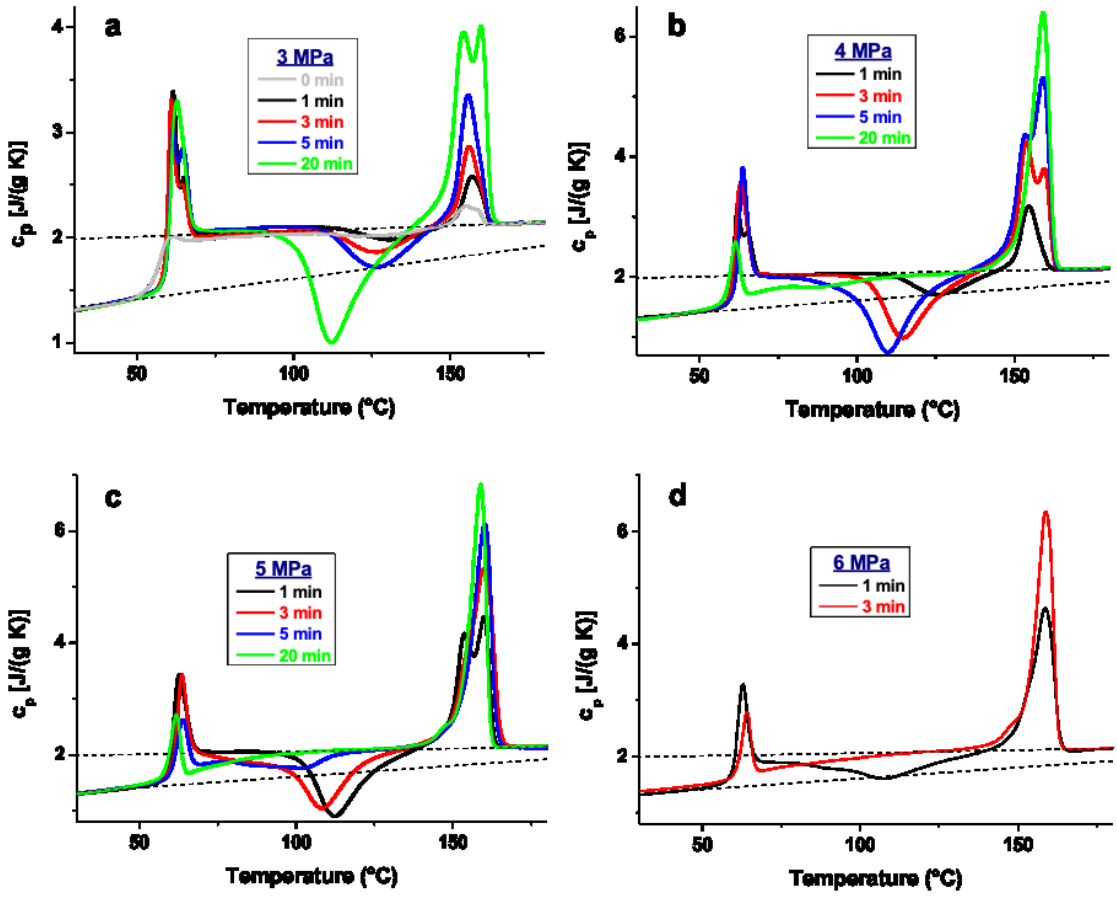

Figure 4 (a, b, c, d). Specific heat capacity (c_p) of PLLA treated with CO_2 at the indicated pressures and t_s, then desorbed, upon heating at 20 K min^{-1}. The dashed lines refer to thermodynamic heat capacity of solid and liquid PLLA.

When heated at 20 K·min^{-1}, quenched PLLA, not exposed to CO_2 (grey curve of Figure 4a) shows the typical T_g of amorphous PLLA around 60°C, coupled to a barely visible enthalpy relaxation exotherm, due to different cooling and heating rates [70]. This is followed by a weak and broad exotherm centered at 130°C and an endotherm peaked at 155°C. Comparison between the cold crystallization exotherm and the melting peak confirms that cooling at 100 K min^{-1} is sufficient to achieve fully amorphous PLLA for this specific grade [40].

Exposure to CO_2 for a few minutes leads to a sizable variation of thermal properties. Starting with *PLLA_3 MPa* (Figure 4a), the glass transition moves to slightly higher temperatures compared to amorphous PLLA. The heat capacity step at T_g is typical of the fully amorphous polymer and overlaps with a significant endotherm, which appears resolved into two peaks, more evident in samples exposed to CO_2 for short times. A significant enthalpy relaxation was expected for all samples, as they had been stored at room temperature

for at least one month prior to the tests [70,71]. A double endotherm in the T_g range has been reported in semicrystalline PLLA due to the enthalpy relaxation of differently constrained mobile amorphous fractions [72]. However, PLLA exposed to 3.0 MPa CO_2 for up to 20 min develops only minor crystallinity, as also probed by WAXD spectra in Figure 2, therefore differently constrained mobile amorphous fractions cannot be claimed as the basis for the double endotherms of Figure 4.

Literature data indicate that strain-induced PLLA mesophase starts to melt immediately above T_g, displaying a post-T_g endotherm in the DSC heating scan [52,73,74]. A sizable endotherm following T_g was also reported to occur at 40-55 °C in a PLLA/THF (tetrahydrofuran) ε-complex, and ascribed to transition from ε-form to α-crystals [75]. A similar endotherm appearing a few degrees above enthalpy relaxation peak was also reported for PLLA conditioned for a few minutes at 2.0 MPa of CO_2 at 0 °C, and was ascribed to disordering of a mesophase developed in the presence of CO_2 [58]. Therefore, it seems reasonable to attribute the double endotherm observed in the T_g range of *PLLA_3 MPa* to enthalpy relaxation of the mobile amorphous fraction and to melting of the α"-mesophase developed after CO_2 desorption). However, further investigations are needed to support this hypothesis and resolve the two endothermic events. The high temperature endotherm/shoulder increases in size with t_s at 3 MPa, possibly revealing a higher mesophase fraction developed upon longer exposure to CO_2, which corroborates the above hypothesis, then finally merges in a single endotherm, with a barely visible shoulder on the high temperature side for *PLLA_3 MPa_20 min*. Heating above T_g leads to a cold crystallization exotherm, which becomes progressively more intense and is anticipated with t_s. This is then followed by a single or double melting endotherm, depending on the cold crystallization temperature, as typical for PLLA [18,43,76].

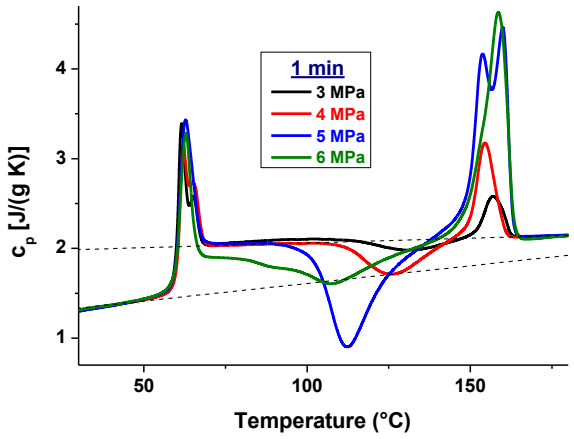

Figure 5. Specific heat capacity (c_p) of PLLA treated with CO_2 for 1 min at the indicated pressures, then desorbed, upon heating at 20 K min^{-1}. The dashed lines refer to thermodynamic heat capacity of solid and liquid PLLA.

A higher CO_2 pressure leads to significant changes in the structure of the PLLA and therefore in the thermal properties, as shown in the thermal analysis graphs of Figure 4. Figure 4b shows how for *PLLA_4*

MPa with t_s < 5 min, the endotherm in the glass transition range appears double-peaked and becomes again more intense with t_s. In *PLLA_4 MPa_20 min*, the glass transition shifts to lower temperatures, and the post-T_g endotherm also reduces in size. For this sample, after 3 months still a minor amount of CO_2 remains within the polymer (< 0.1 mg, corresponding to a weight fraction < 0.007) plasticizing it [64]. Moreover, the cold crystallization exotherms are more intense with increasing t_s, for PLLA exposed to 4.0 MPa of CO_2 for 1 - 5 min, and become almost barely visible in *PLLA_4 MPa_20min*. The latter sample appears semicrystalline upon thermal analysis, as disclosed by the reduction in heat capacity step at T_g, due to the lower mobile amorphous fraction, and by the sizable melting endotherm that is peaked at about 160 °C. Further increase in CO_2 pressure results in faster and more intense cold crystallization exotherm at same t_s (5.0 MPa, 1 - 3 min), which can be better evidenced by comparing the thermal properties of PLLA fixing t_s at 1 min and varying the pressure, as presented in Figure 5. Increasing CO_2 pressure leads to partial crystallization of PLLA at shorter times (5.0 MPa, 5 - 20 min; 6.0 MPa, 1 - 3 min), as also disclosed by FTIR spectra in Figure 3. For *PLLA_6 MPa_3 min*, thermal analysis reveals a significant melting endotherm, and no cold crystallization peak is detected, indicating an initially semicrystalline sample that does not further crystallize upon heating. Its semicrystalline nature is also evidenced by the shift in the mesomorphic/crystalline band from 918 to 921 cm^{-1} in the FTIR-ATR spectrum of Figure 3, suggesting crystal formation during CO_2 treatment. In general, an increase in CO_2 pressure determines an increase in gas sorption rates and gas concentration within the polymer [77]. Then, an increase in gas pressure improves chain mobility and reorganization, with the initial development of a mesophase, followed by the formation of more stable crystals at high CO_2 pressures and sorption times.

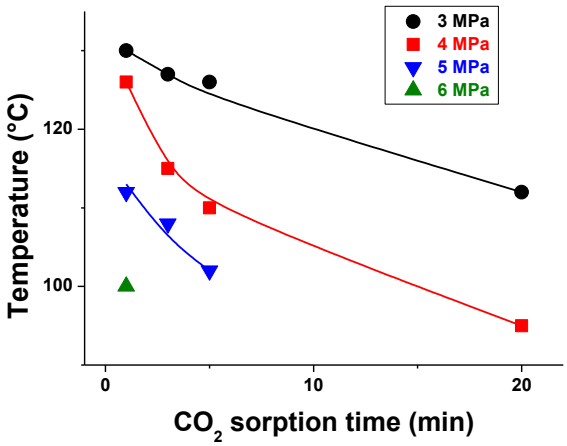

Figure 6. Peak temperatures of cold crystallization exotherms (T_c) of PLLA after CO_2 conditioning at the indicated pressures, as a function of t_s. Lines guide the eye. Data are derived from the DSC curves shown in Figure 4.

The effect of CO_2 treatment on the kinetics of cold crystallization, measured as the exothermic peak temperature (T_c) of the DSC plots of Figure 4, is summarized in Figure 6. An increase in pressure and t_s clearly leads to faster cold crystallization. The variation in crystallization rate is remarkable: in *PLLA_6 MPa_1 min*,

T_c is lowered by about 30 K compared *to PLLA_3.0 MPa_1 min*. Maintaining PLLA under CO_2 for short times (few minutes) can lead to a significant increase in the crystallization rate, as attested by the sizably anticipated T_c. However, the maximum exposure time to CO_2 before the sample crystallizes during treatment reduces with CO_2 pressure; therefore, fine-tuning of the crystallization kinetics is limited. For t_s greater than 1 min under 6.0 MPa of CO_2, or 5 min for a pressure of 5.0 MPa, the polymer crystallizes within the batch autoclave, which limits the adjustment of crystallization kinetics under higher pressures. By increasing t_s, the lowest T_c of 95°C is reached for *PLLA_4 MPa_ 20 min*, which, however, is also accompanied by significant partial crystallization.

The fraction of sample crystallized in the autoclave was estimated by comparing the enthalpy of melting (ΔH_m) and enthalpy of cold crystallization (ΔH_c), measured by integrating the corresponding endothermic/exothermic peaks of the DSC plots shown in Figure 4. Data are presented in Figure 7 as a function of t_s. The exact crystal fraction was not estimated, because in this temperature range both α'- and α-crystals of PLLA develop [43,44,46,47] and the two polymorphs have a largely different enthalpy of melting [78]. For all samples, a ΔH_m - ΔH_c value higher than 0 is measured, which provides quantitative data on the melting of crystals grown in the autoclave, in addition to cold crystallization and melting of the crystals formed upon DSC heating. Mild treatment of PLLA with CO_2 leads not only to growth of the mesophase, but also to the formation of ordered crystals, whose amounts depend on pressure and t_s. This is particularly evident after CO_2 sorption at high pressures, such as 5.0 or 6.0 MPa, with, as an example, a value of $\Delta H_m - \Delta H_c$ that equals to 22 $J \cdot g^{-1}$ for *PLLA_6 MPa_1 min*. Samples conditioned with 4.0 MPa of CO_2 show an initial absence of crystals developed during CO_2 treatment, with $\Delta H_m - \Delta H_c$ values increasing with t_s. On the contrary, treatment with a pressure of 3.0 MPa leads to a minor, if any, growth of crystals within the autoclave, as demonstrated by the low values of ΔH_m - ΔH_c, even for the highest t_s tested.

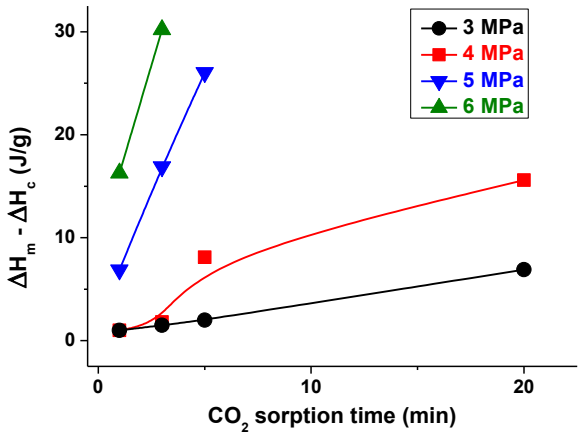

Figure 7. $\Delta H_m - \Delta H_c$ of PLLA after CO_2 treatment at the indicated pressures, as a function of t_s. Data were derived from DSC curves presented in Figure 4. Lines guide the eye

It should be noted that the cold crystallization of PLLA is also enhanced in samples that initially did not contain a sizable initial crystallinity (3.0 – 4.0 MPa, 1 min), but only a small fraction of mesophase; this is

evidenced in Figures 4 and 5 by a sizable cold crystallization exotherm, much larger than that of the amorphous polymer. Similar to strain-induced mesophase [47, 52], also α"-mesophase developed in the presence of CO_2, even if melted at the completion of T_g, accelerates subsequent crystal growth in PLLA. It is likely that some partially ordered or not fully relaxed chain clusters remain after melting the mesomorphic structure, which can facilitate subsequent crystal formation. Memory effects of partially ordered chain segments that, after their melting, can facilitate additional crystal growth have been probed for a number of semicrystalline polymers, including isotactic polypropylene [79], poly(ε-caprolactone) [79], poly(butylene terephthalate) [80, 81], or poly[(R)-3-hydroxybutyrate] [82], to name a few. However, the influence of small amounts of ordered crystals in promoting further crystal growth upon heating, and the exact structure evolution upon heating are still under investigation and will be detailed in a forthcoming manuscript.

Conclusions

PLLA slabs with a thickness of 0.5 mm were treated with a CO_2 pressure of 3.0 to 6.0 MPa at room temperature for 1 - 20 minutes, to study the influence of α"-mesophase on thermal properties and crystallization kinetics of PLLA. The adopted mild CO_2 treatment leads to a small amount of gas dissolved within the polymer, resulting in a limited fraction of mesophase, but its formation can be evidenced even after exposure to CO_2 for very short times (1 - 3 min). The fraction of developed mesophase depends on the CO_2 pressure and sorption time, with prolonged exposure to CO_2 that also leads to the formation of ordered crystals. When the polymer is conditioned with CO_2 at 6.0 MPa, 3 min are sufficient to develop α-crystals. This points to the upper limit for the growth of the mesophase at ambient temperature when a CO_2 pressure of 6.0 MPa is used, at least for the specific grade and thickness of the PLLA used.

The thermal properties of PLLA containing α"-mesophase were studied by DSC, in dependence on both t_s and CO_2 pressure. Cold crystallization of PLLA is enhanced by the initial presence of the mesophase, although it melts at the completion of T_g. The cold crystallization peak temperature T_c is sizably anticipated by increasing CO_2 sorption pressure and time, indicating that a larger mesophase fraction attained with higher CO_2 concentrations within the sample leads to faster reorganization to α-crystals.

The mild CO_2 treatment detailed here may provide the basis for a novel, cost-effective and green process to tune the thermal properties of PLLA. The short time and low pressures needed to reach highly enhanced crystallization rates pave the way for a methodology to widen PLLA application by easy change in processing conditions in a few minutes and with a reduced amount of gas, with the added value of a tuning of properties at a controllable level.

Acknowledgements

The authors thank Total Corbion (The Netherlands) for kindly providing PLLA and Prof. Paolo Aprea of DICMaPI UniNa for his assistance with WAXD analyses.

This article is dedicated to the memory of Prof. Berhnard Wunderlich, a pioneer educator and scientist. MLDL had the wonderful opportunity to work directly under his guidance at the University of Tennessee, where she was introduced by an unsurpassed mentor into the world of Thermal Analysis of Polymers.

References

[1] J.W. Leenslag, A.J. Pennings, R.R.M. Bos, F.R. Rozema, G. Boering, Resorbable materials of poly (L-lactide): VII. In vivo and in vitro degradation, Biomaterials. 8 (1987) 311–314. https://doi.org/10.1016/0142-9612(87)90121-9

[2] J.W. Leenslag, A.J. Pennings, R.R.M. Bos, F.R. Rozema, G. Boering, Resorbable materials of poly (L-lactide). VI. Plates and screws for internal fracture fixation, Biomaterials. 8 (1987) 70–73. https://doi.org/10.1016/0142-9612(87)90034-2

[3] R.A. Gross, B. Kalra, Biodegradable polymers for the environment, Science. 297 (2002) 803–807. https://doi.org/10.1126/science.297.5582.803

[4] D. Garlotta, A literature review of poly (lactic acid), J. Polym. Environ. 9 (2001) 63–84. https://doi.org/10.1023/A:1020200822435

[5] R. Auras, B. Harte, S. Selke, An overview of polylactides as packaging materials, Macromol. Biosci. (2004). https://doi.org/10.1002/mabi.200400043.

[6] J.-W. Rhim, H.-M. Park, C.-S. Ha, Bio-nanocomposites for food packaging applications, Prog. Polym. Sci. 38 (2013) 1629–1652. https://doi.org/10.1016/j.progpolymsci.2013.05.008

[7] T. Iwata, Y. Doi, Morphology and enzymatic degradation of poly (L-lactic acid) single crystals, Macromolecules. 31 (1998) 2461–2467. https://doi.org/10.1021/ma980008h

[8] G. Liu, X. Zhang, D. Wang, Tailoring crystallization: towards high-performance poly (lactic acid), Adv. Mater. 26 (2014) 6905–6911. https://doi.org/10.1002/adma.201305413

[9] H. Bai, C. Huang, H. Xiu, Q. Zhang, H. Deng, K. Wang, F. Chen, Q. Fu, Significantly improving oxygen barrier properties of polylactide via constructing parallel-aligned shish-kebab-like crystals with well-interlocked boundaries, Biomacromolecules. 15 (2014) 1507–1514. https://doi.org/10.1021/bm500167u

[10] H. Cai, V. Dave, R.A. Gross, S.P. McCarthy, Effects of physical aging, crystallinity, and orientation on the enzymatic degradation of poly (lactic acid), J. Polym. Sci. Part B Polym. Phys. 34 (1996) 2701–2708. https://doi.org/10.1002/(SICI)1099-0488(19961130)34:16%3C2701::AID-POLB2%3E3.0.CO;2-S

[11] A.M. Harris, E.C. Lee, Improving mechanical performance of injection molded PLA by controlling crystallinity, J. Appl. Polym. Sci. 107 (2008) 2246–2255. https://doi.org/10.1002/app.27261

[12] M.L. Di Lorenzo, M. Cocca, M. Malinconico, Crystal polymorphism of poly(L-lactic acid) and its influence on thermal properties, Thermochim. Acta. (2011). https://doi.org/10.1016/j.tca.2010.12.027.

[13] M. Cocca, M.L. Di Lorenzo, M. Malinconico, V. Frezza, Influence of crystal polymorphism on mechanical and barrier properties of poly(L-lactic acid), Eur. Polym. J. (2011). https://doi.org/10.1016/j.eurpolymj.2011.02.009.

[14] M. Cocca, R. Androsch, M.C. Righetti, M. Malinconico, M.L. Di Lorenzo, Conformationally disordered crystals and their influence on material properties: The cases of isotactic polypropylene,

isotactic poly(1-butene), and poly(L-lactic acid), J. Mol. Struct. (2014). https://doi.org/10.1016/j.molstruc.2014.02.038.

[15] G. Perego, G.D. Cella, C. Bastioli, Effect of molecular weight and crystallinity on poly (lactic acid) mechanical properties, J. Appl. Polym. Sci. 59 (1996) 37–43. https://doi.org/10.1002/(SICI)1097-4628(19960103)59:1%3C37::AID-APP6%3E3.0.CO;2-N

[16] M.L. Di Lorenzo, R. Androsch, Industrial Applications of Poly(lactic acid), Vol. 282. Cham: Springer, 2018. https://doi.org/10.1007/978-3-319-75459-8

[17] D. da Silva, M. Kaduri, M. Poley, O. Adir, N. Krinsky, J. Shainsky-Roitman, A. Schroeder, Biocompatibility, biodegradation and excretion of polylactic acid (PLA) in medical implants and theranostic systems, Chem. Eng. J. 340 (2018) 9–14. https://doi.org/https://doi.org/10.1016/j.cej.2018.01.010.

[18] R. Androsch, M.L. Di Lorenzo, C. Schick, Kinetics of Nucleation and Growth of Crystals of Poly(L-lactic) acid, in: M.L. Di Lorenzo, R. Androsch (Eds.) Synthesis, Structure and Properties of Poly(lactic acid). Advances in Polymer Science, vol 279. Springer, Cham, 2017, pp. 235–272. https://doi.org/10.1007/12_2016_13

[19] S. Saeidlou, M.A. Huneault, H. Li, C.B. Park, Poly (lactic acid) crystallization, Prog. Polym. Sci. 37 (2012) 1657–1677. https://doi.org/10.1016/j.progpolymsci.2012.07.005

[20] H. Tsuji, Quiescent Crystallization of Poly (Lactic Acid) and Its Copolymers-Based Materials, In: M.L. Di Lorenzo, R. Androsch (Eds.) Thermal Properties of Bio-based Polymers. Advances in Polymer Science, vol 283. Springer, Cham, 2019, pp. 37–86. https://doi.org/10.1007/12_2019_46

[21] R. Androsch, M.L. Di Lorenzo, Crystal nucleation in glassy poly(L-lactic acid), Macromolecules. (2013). https://doi.org/10.1021/ma401036j.

[22] M.L. Di Lorenzo, P. Rubino, R. Luijkx, M. Hélou, Influence of chain structure on crystal polymorphism of poly(lactic acid). Part 1: Effect of optical purity of the monomer, Colloid Polym. Sci. (2014). https://doi.org/10.1007/s00396-013-3081-z.

[23] M.L. Di Lorenzo, P. Rubino, B. Immirzi, R. Luijkx, M. Hélou, R. Androsch, Influence of chain structure on crystal polymorphism of poly (lactic acid). Part 2. Effect of molecular mass on the crystal growth rate and semicrystalline morphology, Colloid Polym. Sci. 293 (2015) 2459–2467. https://doi.org/10.1007/s00396-015-3709-2

[24] C. Zhao, D. Wu, N.A.N. Huang, H. Zhao, Crystallization and thermal properties of PLLA comb polymer, J. Polym. Sci. Part B Polym. Phys. 46 (2008) 589–598. https://doi.org/10.1002/polb.21394

[25] M.L. Di Lorenzo, R. Androsch, Synthesis, Structure and Properties of Poly (lactic acid), Vol. 279. Cham: Springer, 2018. https://doi.org/10.1007/978-3-319-64230-7.

[26] H. Li, M.A. Huneault, Effect of nucleation and plasticization on the crystallization of poly(lactic acid), Polymer (Guildf). 48 (2007) 6855–6866. https://doi.org/https://doi.org/10.1016/j.polymer.2007.09.020.

[27] M.L. Di Lorenzo, A. Longo, N, N-Diethyl-3-methylbenzamide (DEET): A mosquito repellent as

functional plasticizer for poly (L-lactic acid), Thermochim. Acta. 677 (2019) 180–185. https://doi.org/10.1016/j.tca.2019.02.004

[28] I. Bonadies, A. Longo, R. Androsch, M.L. Di Lorenzo, Biodegradable electrospun PLLA fibers containing the mosquito-repellent DEET, Eur. Polym. J. 113 (2019) 377–384. https://doi.org/10.1016/j.eurpolymj.2019.02.001.

[29] M. Penco, G. Spagnoli, I. Peroni, M.A. Rahman, M. Frediani, W. Oberhauser, A. Lazzeri, Effect of nucleating agents on the molar mass distribution and its correlation with the isothermal crystallization behavior of poly (L-lactic acid), J. Appl. Polym. Sci. 122 (2011) 3528–3536. https://doi.org/10.1002/app.34761

[30] A. Pei, Q. Zhou, L.A. Berglund, Functionalized cellulose nanocrystals as biobased nucleation agents in poly (L-lactide)(PLLA)–Crystallization and mechanical property effects, Compos. Sci. Technol. 70 (2010) 815–821. https://doi.org/10.1016/j.compscitech.2010.01.018

[31] S. Sharma, A. Majumdar, B.S. Butola, Tailoring the biodegradability of polylactic acid (PLA) based films and ramie-PLA green composites by using selective additives, Int. J. Biol. Macromol. 181 (2021) 1092–1103. https://doi.org/10.1016/j.ijbiomac.2021.04.108

[32] M. Nofar, A. Tabatabaei, A. Ameli, C.B. Park, Comparison of melting and crystallization behaviors of polylactide under high-pressure CO_2, N_2, and He, AIP Conf. Proc. 1593 (2014) 320–323. https://doi.org/10.1063/1.4873791.

[33] M. Nofar, W. Zhu, C.B. Park, Effect of dissolved CO_2 on the crystallization behavior of linear and branched PLA, Polymer (Guildf). 53 (2012) 3341–3353. https://doi.org/10.1016/j.polymer.2012.04.054.

[34] L. Yu, H. Liu, K. Dean, Thermal behaviour of poly(lactic acid) in contact with compressed carbon dioxide, Polym. Int. 58 (2009) 368–372. https://doi.org/10.1002/pi.2540.

[35] Y.-M. Corre, A. Maazouz, J. Reignier, J. Duchet, Influence of the chain extension on the crystallization behavior of polylactide, Polym. Eng. & Sci. 54 (2014) 616–625. https://doi.org/https://doi.org/10.1002/pen.23595.

[36] N. Burgos, D. Tolaguera, S. Fiori, A. Jiménez, Synthesis and characterization of lactic acid oligomers: Evaluation of performance as poly (lactic acid) plasticizers, J. Polym. Environ. 22 (2014) 227–235. https://doi.org/10.1007/s10924-013-0628-5

[37] M.L. Di Lorenzo, R. Androsch, Accelerated crystallization of high molar mass poly (L/D-lactic acid) by blending with low molar mass poly (L-lactic acid), Eur. Polym. J. 100 (2018) 172–177. https://doi.org/10.1016/j.eurpolymj.2018.01.030

[38] B. Wunderlich, Macromolecular Physics, Crystal Nucleation, Growth, Annealing, Vol. 2, Academic Press, New York, 1976.

[39] C. Schick, R. Androsch, J.W.P. Schmelzer, Homogeneous crystal nucleation in polymers, J. Phys. Condens. Matter. 29 (2017) 453002. https://doi.org/10.1088/1361-648X/aa7fe0

[40] A. Longo, E. Di Maio, M.L. Di Lorenzo, Heterogeneous Bubble Nucleation by Homogeneous Crystal

Nuclei in Poly (L-Lactic Acid) Foaming, Macromol. Chem. Phys. 223 (2022) 2100428. https://doi.org/10.1002/macp.202100428

[41] A. Longo, G. Dal Poggetto, M. Malinconico, P. Laurienzo, E. Di Maio, M.L. Di Lorenzo, Enhancement of crystallization kinetics of poly(L-lactic acid) by grafting with optically pure branches, Polymer (Guildf). 227 (2021) 123852. https://doi.org/https://doi.org/10.1016/j.polymer.2021.123852.

[42] N. Najafi, M.-C. Heuzey, P. Carreau, D. Therriault, Quiescent and shear-induced crystallization of linear and branched polylactides, Rheol. Acta. 54 (2015) 831–845. https://doi.org/10.1007/s00397-015-0874-7

[43] M.L. Di Lorenzo, R. Androsch, Influence of α′-/α-crystal polymorphism on properties of poly(L-lactic acid), Polym. Int. (2019). https://doi.org/10.1002/pi.5707.

[44] M.L. Di Lorenzo, R. Androsch, Crystallization of Poly(lactic acid), in: Biodegrad. Polyesters, John Wiley & Sons, Ltd, 2015: pp. 109–130. https://doi.org/https://doi.org/10.1002/9783527656950.ch5.

[45] L. Cartier, T. Okihara, Y. Ikada, H. Tsuji, J. Puiggali, B. Lotz, Epitaxial crystallization and crystalline polymorphism of polylactides, Polymer https://doi.org/10.1016/S0032-3861(00)00234-2. 41 (2000) 8909–8919.

[46] B. Lotz, Crystal polymorphism and morphology of polylactides, In: M.L. Di Lorenzo, R. Androsch (Eds-) Synthesis, Structure and Properties of Poly(lactic acid). Advances in Polymer Science, vol 279. Springer, Cham, 2017: pp. 273–302. https://doi.org/10.1007/12_2016_15.

[47] Y. Zheng, P. Pan, Crystallization of biodegradable and biobased polyesters: Polymorphism, cocrystallization, and structure-property relationship, Prog. Polym. Sci. 109 (2020) 101291. https://doi.org/10.1016/j.progpolymsci.2020.101291

[48] J.P. Kalish, K. Aou, X. Yang, S.L. Hsu, Spectroscopic and thermal analyses of α′ and α crystalline forms of poly (L-lactic acid), Polymer. 52 (2011) 814–821. https://doi.org/10.1016/j.polymer.2010.12.042

[49] H. Marubayashi, S. Asai, M. Sumita, Crystal structures of poly (L-lactide)–CO_2 complex and its emptied form, Polymer. 53 (2012) 4262–4271. https://doi.org/10.1016/j.polymer.2012.07.044

[50] H. Marubayashi, S. Asai, M. Sumita, Guest-induced crystal-to-crystal transitions of Poly (L-lactide) complexes, J. Phys. Chem. B. 117 (2013) 385–397. https://doi.org/10.1021/jp308999t

[51] Y. Zheng, C.-L. Zhang, Y.-Z. Bao, G.-R. Shan, P.-J. Pan, Temperature-dependent Crystallization and Phase Transition of Poly (L-lactic acid)/CO_2 Complex Crystals, Chinese J. Polym. Sci. 39 (2021) 484–492. https://doi.org/10.1007/s10118-021-2502-6

[52] G. Stoclet, R. Seguela, J.-M. Lefebvre, C. Rochas, New Insights on the Strain-Induced Mesophase of Poly(D,L-lactide): In Situ WAXS and DSC Study of the Thermo-Mechanical Stability, Macromolecules. 43 (2010) 7228–7237. https://doi.org/10.1021/ma101430c.

[53] G. Stoclet, R. Seguela, J.-M. Lefebvre, S. Elkoun, C. Vanmansart, Strain-induced molecular ordering in polylactide upon uniaxial stretching, Macromolecules. 43 (2010) 1488–1498.

https://doi.org/10.1021/ma9024366

[54] J. Hu, T. Zhang, M. Gu, X. Chen, J. Zhang, Spectroscopic analysis on cold drawing-induced PLLA mesophase, Polymer. 53 (2012) 4922–4926. https://doi.org/10.1016/j.polymer.2012.09.012

[55] J. Zhang, Y. Duan, A.J. Domb, Y. Ozaki, PLLA Mesophase and Its Phase Transition Behavior in the PLLA−PEG−PLLA Copolymer As Revealed by Infrared Spectroscopy, Macromolecules. 43 (2010) 4240–4246. https://doi.org/10.1021/ma100301h.

[56] T. Zhang, J. Hu, Y. Duan, F. Pi, J. Zhang, Physical Aging Enhanced Mesomorphic Structure in Melt-Quenched Poly(L-lactic acid), J. Phys. Chem. B. 115 (2011) 13835–13841. https://doi.org/10.1021/jp2087863.

[57] Q. Lan, Y. Li, Mesophase-Mediated Crystallization of Poly(L-lactide): Deterministic Pathways to Nanostructured Morphology and Superstructure Control, Macromolecules. 49 (2016) 7387–7399. https://doi.org/10.1021/acs.macromol.6b01442.

[58] Q. Lan, Y. Li, H. Chi, Highly Enhanced Mesophase Formation in Glassy Poly(L-lactide) at Low Temperatures by Low-Pressure CO_2 That Provides Moderately Increased Molecular Mobility, Macromolecules. 49 (2016) 2262–2271. https://doi.org/10.1021/acs.macromol.6b00044.

[59] H. Marubayashi, S. Akaishi, S. Akasaka, S. Asai, M. Sumita, Crystalline structure and morphology of poly(L-lactide) Formed under high-pressure CO_2, Macromolecules. 41 (2008) 9192–9203. https://doi.org/10.1021/ma800766h.

[60] S. Li, T. Chen, X. Liao, W. Han, Z. Yan, J. Li, G. Li, Effect of Macromolecular Chain Movement and the Interchain Interaction on Crystalline Nucleation and Spherulite Growth of Polylactic Acid under High-Pressure CO_2, Macromolecules. 53 (2020) 312–322. https://doi.org/10.1021/acs.macromol.9b01601.

[61] X. Liao, A. V Nawaby, The sorption behaviors in PLLA-CO_2 system and its effect on foam morphology, J. Polym. Res. 19 (2012) 1–9. https://doi.org/10.1007/s10965-012-9827-3

[62] Luminy® PLA neat resins, https://totalcorbion.4net-acc.com/media/iufhvey2/factsheet_luminy-pla-neat-resins_20190903.pdf (accessed 2 September 2022).

[63] D. Tammaro, V. Contaldi, M.G.P. Carbone, E. Di Maio, S. Iannace, A novel lab-scale batch foaming equipment: The mini-batch, J. Cell. Plast. 52 (2016) 533–543. https://doi.org/10.1177/0021955X15584654.

[64] Q. Lan, J. Yu, J. He, F.H.J. Maurer, J. Zhang, Thermal behavior of poly (L-lactide) having low L-isomer content of 94% after compressed CO_2 treatment, Macromolecules. 43 (2010) 8602–8609. https://doi.org/10.1021/ma101473r

[65] S. Sarge, W. Hemminger, E. Gmelin, G. Höhne, H. Cammenga, W. Eysel, Metrologically based procedures for the temperature, heat and heat flow rate calibration of DSC, J. Therm. Anal. Calorim. 49 (1997) 1125–1134. https://doi.org/10.1007/BF01996802

[66] J. Zhang, Y. Duan, H. Sato, H. Tsuji, I. Noda, S. Yan, Y. Ozaki, Crystal modifications and thermal behavior of poly (L-lactic acid) revealed by infrared spectroscopy, Macromolecules. 38 (2005) 8012–

8021. https://doi.org/10.1021/ma051232r

[67] B. Xue, L. Xie, J. Zhang, Detailed molecular movements during poly (L-lactic acid) cold-crystallization investigated by FTIR spectroscopy combined with two-dimensional correlation analysis, RSC Adv. 7 (2017) 47017–47028. https://doi.org/10.1039/C7RA08921J

[68] V. Krikorian, D.J. Pochan, Crystallization behavior of poly (L-lactic acid) nanocomposites: nucleation and growth probed by infrared spectroscopy, Macromolecules. 38 (2005) 6520–6527.

[69] P. Larkin, Instrumentation and Sampling Methods, in: P. Larkin (Ed.), Infrared Raman Spectrosc., Elsevier, Oxford, 2011: pp. 27–54. https://doi.org/https://doi.org/10.1016/B978-0-12-386984-5.10003-5.

[70] B. Wunderlich, Thermal analysis of polymeric materials, Springer Berlin, Heidelberg, 2005. https://doi.org/10.1007/b137476

[71] X. Monnier, D. Cavallo, M.C. Righetti, M.L. Di Lorenzo, S. Marina, J. Martin, D. Cangialosi, Physical aging and glass transition of the rigid amorphous fraction in poly (L-lactic acid), Macromolecules. 53 (2020) 8741–8750. https://doi.org/10.1021/acs.macromol.0c01182

[72] M.C. Righetti, Amorphous Fractions of Poly (lactic acid), In: Di Lorenzo, M., Androsch, R. (eds) Synthesis, Structure and Properties of Poly(lactic acid). Advances in Polymer Science, vol 279. Springer, Cham, 2017, pp. 195–234. https://doi.org/10.1007/12_2016_14.

[73] R. Lv, B. Na, N. Tian, S. Zou, Z. Li, S. Jiang, Mesophase formation and its thermal transition in the stretched glassy polylactide revealed by infrared spectroscopy, Polymer. 52 (2011) 4979–4984. https://doi.org/10.1016/j.polymer.2011.08.023

[74] Y. Wang, L. Liu, M. Li, W. Cao, C. Liu, C. Shen, Spectroscopic analysis of post drawing relaxation in poly (lactic acid) with oriented mesophase, Polym. Test. 43 (2015) 103–107. https://doi.org/10.1016/j.polymertesting.2015.03.001

[75] N.M. Praveena, P. Shaiju, R.B.A. Raj, E.B. Gowd, Infrared bands to distinguish amorphous, meso and crystalline phases of poly (lactide) s: Crystallization and phase transition pathways of amorphous, meso and co-crystal phases of poly (L-lactide) in the heating process, Polymer. 240 (2022) 124495. https://doi.org/10.1016/j.polymer.2021.124495

[76] M.L. Di Lorenzo, R. Androsch, Stability and Reorganization of α′-Crystals in Random L/D-Lactide Copolymers, Macromol. Chem. Phys. (2016). https://doi.org/10.1002/macp.201600073.

[77] G. Li, H. Li, L.S. Turng, S. Gong, C. Zhang, Measurement of gas solubility and diffusivity in polylactide, Fluid Phase Equilib. 246 (2006) 158–166. https://doi.org/10.1016/j.fluid.2006.05.030

[78] M.C. Righetti, M. Gazzano, M.L. Di Lorenzo, R. Androsch, Enthalpy of melting of α′-and α-crystals of poly (L-lactic acid), Eur. Polym. J. 70 (2015) 215–220. https://doi.org/10.1016/j.eurpolymj.2015.07.024

[79] A.T. Lorenzo, M.L., Arnal, J.J. Sánchez, A.J. Müller, A.J., Effect of annealing time on the self-nucleation behavior of semicrystalline polymers. J. Polym. Sci. B Polym. Phys. 44 (2006) 1738-1750. https://doi.org/10.1002/polb.20832

[80] M.L. Di Lorenzo, M.C., Righetti, Morphological analysis of poly(butylene terephthalate) spherulites during fusion. Polym. Bull. 53 (2004) 53–62. https://doi.org/10.1007/s00289-004-0315-8

[81] M.L. Di Lorenzo, M.C., Righetti, M. Angiui, E. Tombari, Structural reorganization in poly(butylene terephthalate) during fusion, Macromolecules 37 (2004) 9027–9033. https://doi.org/10.1021/ma0492667

[82] M.L. Di Lorenzo, P. Sajkiewicz, A. Gradys, P. La Pietra, Optimization of melting conditions for the analysis of crystallization kinetics of poly(3-hydroxybutyrate), e-Polymers2009, no.027. https://doi.org/10.1515/epoly.2009.9.1.313